Pattern selection in an anisotropic Hele-Shaw cell

K. V. McCloud and J. V. Maher
Department of Physics and Astronomy, University of Pittsburgh, Pittsburgh, Pennsylvania 15260
(Received 31 May 1994)

The selection of steady-state viscous fingers has been measured in Hele-Shaw cells that are perturbed by having rectangular and square lattices etched on one of their plates. The strength of the perturbation was varied by varying the cell gap, and over a wide range of observable tip velocities this local perturbation was also made microscopic in the sense that the capillary length of the flow was large in comparison to the cell size of the underlying lattice. Above threshold the microscopic perturbation results in the selection of wider fingers than those selected in the unperturbed flow for all channel orientations in the experiment. All observed solutions are symmetric, centered in the channel, and have the relation between tip curvature and finger width expected of members of the Saffman-Taylor family of solutions. Selected solutions narrow again at tip velocities where the perturbations can no longer be considered microscopic.

PACS number(s): 47.20.−k, 68.10.−m

INTRODUCTION

Saffman-Taylor (ST) flow, the motion of an interface between immiscible fluids in a rectangular Hele-Shaw cell, is a particularly simple example of a nonlinear, pattern-forming system. The steady-state viscous finger formed in such a system, whose selection from a family of possible solutions has only recently been explained [1–3], has been studied in detail [4–7]. Using this steady-state finger as a starting point, it should be possible to learn more about nonlinear growth laws by perturbing the system in a well-controlled fashion. Recently, there have been a number of experiments involving perturbed flows in both rectangular and radial Hele-Shaw cells. Most of these have involved placing wires, grooves, or bubbles near the tip of a growing finger [8–15]. Most available results on flow over a lattice have used the radial Hele-Shaw geometry [16–18], gaining richness in the patterns observed but sacrificing the simplicity of the steady state, which is unique to the channel geometry. In the channel geometry, the experiments performed so far have all involved macroscopic perturbations in the sense that the imposed length scale of the perturbation is greater than the capillary length of the flow [8, 11, 12, 14, 19–21]. In most of these cases, the selected finger tends to be narrower and much more stable than the unperturbed solution. The available theoretical work also tends to favor the selection of narrow fingers in the case of general anisotropy added by the imposed perturbation [21–32] . One interesting experimental exception involves high-velocity flow over a lattice [19, 21], a flow which exhibits very unstable diffusion-limited-aggregation (DLA)-like fingers, which reflect the symmetry of the underlying lattice. Averaging over a large number of such unstable flows produces an average finger, which has the general shape of a ST finger, but is sometimes wider than the corresponding ST finger should be [19, 21]. In this paper, we present results from an experiment involving stable flow in the channel geometry over a lattice whose cell size is, in general, much smaller than the capillary length of the interfacial flow.

EXPERIMENTAL PROCEDURES AND DATA PRESENTATION

The experimental cells were 50 cm long, with a channel width set by the placement of Teflon spacers which also set the gap, b, between the plates of the cell. The channel width, w, varied from 2 to 5 cm, with most of the data taken at a channel width of 3 cm. Four different values of the gap, b, were used, ranging from 0.37 mm to 1.60 mm. The bottom plate of the cell consisted of a 0.5 inch thick piece of very uniform float glass. The top plate was a 0.5 inch thick piece of glass with a very precise lattice etched into it. Two etched top plates were used, one with a square lattice, and the other with a rectangular lattice. Some calibration data were also measured using a smooth top plate. Lattice specifications are listed in Table I. A flow realization involved injecting nitrogen gas into the cell after filling the cell with heavy paraffin oil (viscosity, $\mu = 180$ cP and surface tension, T=35.4 dye/cm). Only flows with a very constant areal injection rate (variation less than 5% over a 15 cm finger-tip advance) were accepted and analyzed. Each flow was recorded from above using a CCD camera and a medical-grade VCR, and the images were analyzed digitally. Measurements were made of the tip velocities, v, tip curvatures, finger widths, λw, and limits of stability as a function of the cell gap, the lattice geometry, and the angle, θ, between the direction of flow and the symmetry axis of the lattice. While all measured quantities for one flow realization could be established very accurately, repeated measurements showed that the finger width was reproducible to within ±5% and the stability limit to within

TABLE I. The dimensions of the etched lattices are shown here.

Lattice	Depth (μm)	Groove width (μm)	Center to center (μm)
Square	90±5	200±13	400±3 × 400±3
Rectangle	90±5	200±13	400±3 × 800±3

±15% of the dimensionless control parameter, $1/B$ (defined below). Several general features of the fingers were robustly reproducible: (1) The fingers were always symmetric and centered in the channel; (2) even in the cases (to be presented below) where the finger width was much different from the normal ST (unperturbed) finger, the relation between finger width and tip curvature was that expected of a member of the ST family of solutions. That is, the fingers could be fit to the modified zero surface tension ST relation found by Pitts [33],

$$x = \frac{\lambda}{\pi}\ln\frac{1}{2}[1+\cos(\pi y/\lambda)] , \tag{1}$$

with good precision. In this relation y is the position in the direction of the flow channel, x is the position across the channel, we have normalized the half width $w/2$ of the cell to unit length, and the origin is located at the finger tip. This relation is known to fit fingers in the range $0.5 < \lambda < 0.8$ well [33]; (3) at large gaps, the fingers were indistinguishable from normal ST fingers in all respects (width and tip curvature); (4) at low velocities and large gaps, standard velocity-dependent wetting corrections brought the finger into good agreement with previously published results [34]; (5) the limits of stability with large gaps were always comparable to those observed in smooth (no lattice) cells. Below, we present finger widths, λ (fraction of cell width, w, occupied by the fingers), as functions of the dimensionless number,

$$1/B = \frac{12\mu v w^2}{T b^2} . \tag{2}$$

We arbitrarily set the gap, b, to be the gap set by the Teflon spacers plus 1/2 the etching depth of the lattice. The range of uncertainty in the gap introduced by the ambiguity in how much of the etching depth to include in $1/B$ introduces an absolute uncertainty in $1/B$ of as much as 20%, but this is small in comparision to the large effects discussed below. Only relative uncertainty is included in the error bars, and this is negligibly small in $1/B$. Since the oil completely wets the glass plates of the cell, the curvature-dependent pressure jump across the interface in an unperturbed cell can be expressed as a power series in the velocity [35]. For $1/B^* \leq 200$, this power series can be truncated to one nontrivial term, which Tabeling and Libchaber [36] have incorporated into a correction to the surface tension. In this case, the wetting corrected dimensionless number is

$$1/B^* = \frac{12\mu v w^2}{T^* b^2} , \tag{3}$$

where

$$T^* = T[\pi/4 + \alpha\lambda w/b(\mu v/T)^{2/3}] , \tag{4}$$

and α is a constant which, if set to the reasonable value of 1.3, brings our smooth plate and large gap data into very close agreement with the data of Tabeling and Libchaber [36]. While this wetting correction was useful for comparing our low-velocity large-gap data with previously published results and showing that, at large gaps, the lattices have no observable effect on the ST finger, much of the range of data to be discussed below involved tip velocities too high for this correction to be useful. Accordingly, we present results below in the uncorrected form $1/B$. For smaller cell gaps, changes in the finger width and stability from the ST values are observable. The most dramatic changes are observed with the smallest gap, b=0.37 mm. The behavior of the finger width with increasing $1/B$ has several features, which appear in all cases at b=0.37 mm. These features can be illustrated by Figs. 1 and 2 where the finger width, λ, is shown vs $1/B$ for the rectangular lattice (Fig. 1) with the flow channel oriented at three different angles to the symmetry axis of the lattice, and for the square lattice (Fig. 2) with two different channel orientations to the lattice's symmetry axis. At very low tip velocities (low $1/B$), the anisotropy has little or no effect. At only slightly higher velocities, the finger departs dramatically from the smooth ST curve at a sharp angle in the direction of wider fingers. The finger remains unusually wide as $1/B$ is increased until the capillary length, l_c, becomes of the same order as the lattice-cell

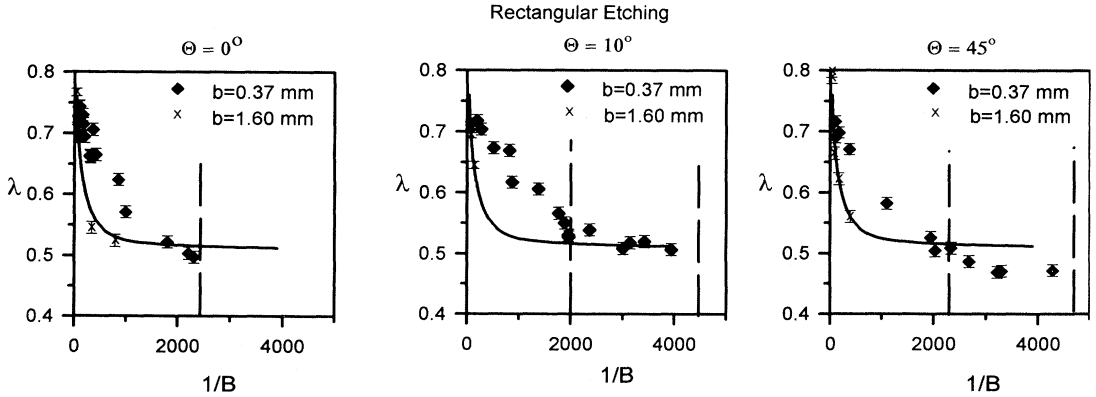

FIG. 1. Rectangular lattice: dimensionless λ vs dimensionless $1/B$ for θ =0°, θ = 10°, and θ = 45° for indicated values of the cell gap, b. The solid curve was sketched through the data shown in Fig. 2 for an unperturbed cell. The right hand (or only) dashed line marks the stability limit for steady-state flow. In the two cases with a second line, the left hand line marks the point, discussed in the text, where an initial wider-finger snaps into a narrower and apparently steady-state finger.

size, d, where the capillary length decreases with velocity and is given by

$$l_c = \frac{Tb}{12\mu v} . \quad (5)$$

In the range $l_c \cong d$, the finger width returns to near the unperturbed ST value. This effect can be seen in both Figs. 1 and 2. Flow over the rectangular lattice at θ=0° and 10° to the symmetry axis of the lattice shows a return to the ST curve, while flow with the same lattice at 45° shows a curve which goes below the ST curve to fingers, which are narrower than the unperturbed ST case. Flow over the square lattice at 0° and 10° stays slightly above the smooth ST curve, as shown in Fig. 2. The limit of stability for the steady-state finger is dramatically dependent on the lattice and flow angle, as well as dependent on the degree of anisotropy. This limit for b=0.37 mm is shown as a vertical line in Figs. 1 and 2 (in cases where there are two vertical lines, the limit at the larger value of $1/B$ is the stability limit). For flow over the square lattice at 0° or 10°, the lowest anisotropy (largest gap) fingers are stable to about $1/B$ = 5000, while the highest anisotropy fingers are only stable up to about $1/B$ = 2500. For the rectangular lattice at 0°, high anisotropy fingers are again stable to about $1/B$=2300, but at 10° and 45°, the fingers are stable to about $1/B$=4500. For a smooth cell, this stability limit arises from macroscopic perturbations in the cell, whose minimum required size shrinks with tip velocity until the irregularities in the cell are enough to destabilize the steady-state finger [37]. Thus the limit depends to some extent on the particular cell used, and we are unable to compare limits measured using two different plates of glass in the cell and confidently relate the stability limits to universal properties. On the other hand, we can confidently compare stability limits, which depend only on changes in anisotropy or angle, and these suggest that flow over either lattice at 0° is very unstable. Figure 3 shows stability limits for all orientations of both lattices as a function of anisotropy (defined as a = etch depth/b). Uncertainties shown in Fig. 3 reflect the range of tip velocities at which instabilities were observed to set in. It should be noted that the present definition of the anisotropy parameter, a, bears no unambiguous relation to the surface tension anisotropy parameter, ϵ, normally used in theoretical formulations of the pattern-forming equations. On the other hand, it is reasonable to assume that the surface tension anisotropy varies monotonically with the parameter a. For the rectangular lattice when the flow direction makes an angle, θ, of 10° and 45° to the lattice's symmetry axis, there is a range of control parameter, $1/B$, in which a wide initial apparent-steady-state sets up, then forms a finger-tip anomaly rather like the beginning of tip splitting, and finally snaps into a narrower and apparently true steady state. These regions of $1/B$ lie between the two vertical lines in the relevant sections of Fig. 1, and the finger widths shown in these sections are the widths of the final steady-state fingers. These regions have only been observed at high anisotropy.

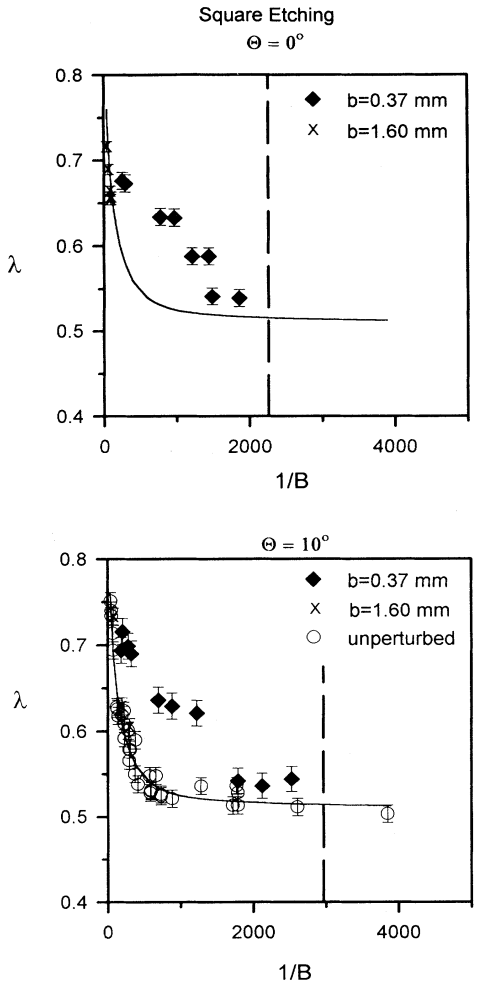

FIG. 2. Square lattice; dimensionless λ vs dimensionless $1/B$ for θ = 0° and θ = 10° for indicated values of the cell gap, b. The solid curve is sketched through the data shown at θ = 10 for an unperturbed cell, and the same curve is shown for all cases here and in Fig. 1. The dashed line marks the stability limit for steady-state flow.

DISCUSSION OF RESULTS

We can suggest a tentative approach to thinking about the results presented above. Sarkar and Jasnow [38] have suggested that if the capillary length is much greater than the lattice-cell size, then it may be legitimate to use a coarse graining argument to represent an otherwise very complicated mobility tensor in Darcy's law:

$$\mathbf{V} = -\underline{\mathbf{M}}\nabla\tilde{\mathbf{P}} , \quad (6)$$

where $\mathbf{V}$ is the interface velocity, $\underline{\mathbf{M}}$ is the coarse grained mobility tensor, and $\tilde{\mathbf{P}}$ is the pressure field averaged over the cell gap. If coarse graining is valid, this mobility tensor should have equal eigenvalues for a lattice with fourfold or sixfold symmetry. In general, the mobility tensor will have unequal eigenvalues for the rectangular lattice. Thus the equation of flow for the square lattice remains a Laplace equation, and that for the rectangular

lattice could change in an important way. We should also consider changes in the boundary conditions. For a smooth cell (no lattice at all), the boundary conditions are that the normal components of velocity for the two fluids must match:

$$(v_n)_1 = (v_n)_2 \ , \tag{7}$$

and that the pressure jump across the two fluids, one of which is assumed to wet the plates, should have the form,

$$\Delta P = \frac{T}{b/2}\left[1 + 3.80\left(\frac{\mu v_n}{T}\right)^{2/3} + \text{higher order terms in } v\right] + \frac{\pi}{4} T\kappa \ , \tag{8}$$

where κ is the curvature in the x-y plane. The presence of the lattice can be expected to change these boundary conditions, and it is not at all clear how to write down the corrected boundary conditions which should reflect the anisotropy. One might expect anisotropy to bring in both an angular dependence to the surface tension T in Eq. (8) and also a kinetic (v_n-dependent) term.

Differences between flows over the square lattice and the rectangular lattice might be attributed to the dynamical equation, but strong similarities between anisotropy-dependent features of the flows can probably be assumed to arise from the boundary conditions. For b=0.37 mm and a channel width of 3 cm, the capillary length is larger than the lattice-cell size for $1/B \leq 2600$. The measured lattice effects on the steady-state finger are very similar for both the square and the rectangular lattice in this range. This is illustrated in Fig. 4 , which shows the ratio of the b=0.37 mm finger's width to the ST finger width for all cases. This strong similarity suggests that the entire wide-finger phenomenon may be attributable to the lattice boundary conditions, with little sensitivity to the

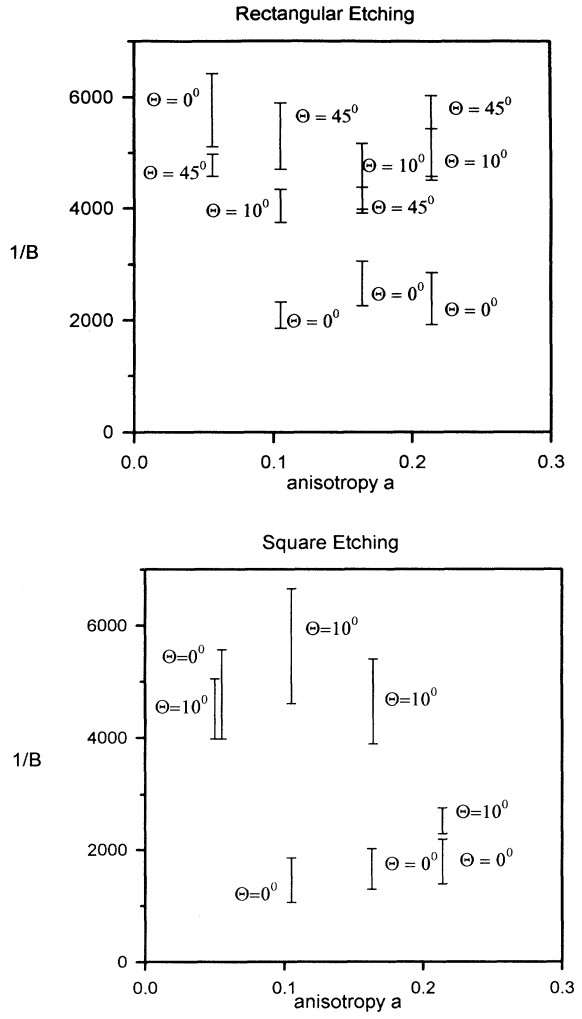

FIG. 3. Stability against tip splitting for all orientations of flow on rectangular and square lattices as a function of the dimensionless anisotropy parameter, a, defined in the text. The vertical line segments give the range of the dimensionless control parameter, $1/B$, within which the fingers have, in at least one flow realization, been observed to become unstable.

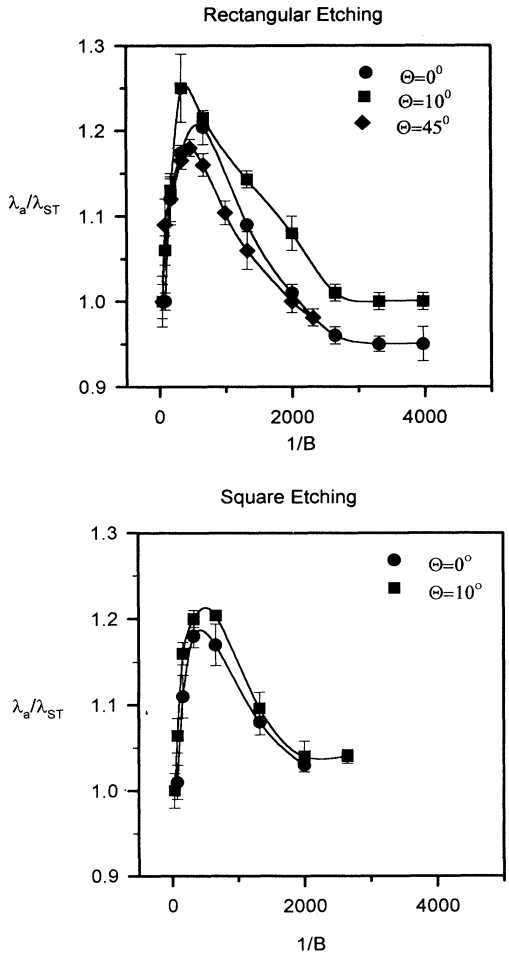

FIG. 4. Dimensionless ratio of perturbed-cell finger width to unperturbed-cell finger width for b=0.42 mm for the rectangular and square lattices at all orientations. The lines shown are sketched to guide the eye.

mobility tensor in the dynamical equation. Strong instability in the square lattice flow at relatively low values of $1/B$ may result from interesting differences in the mobility tensor in the dynamical equation, but these only occur when the capillary length is of the order of the lattice-cell size and, therefore, cannot easily be discussed in the framework of an averaged mobility tensor.

The differences in the finger width at large $1/B$ may result from differences in the mobility tensor in the dynamical equation, but these effects are seen at values of $1/B$, where the capillary length is of the same order or smaller than the lattice-cell size and again cannot be easily discussed in the framework of an averaged mobility tensor. Such finger-width effects, with fatter fingers at some orientations, θ, and thinner fingers at others, may be understandable in terms of the previously available literature [21–23, 25, 31, 32], although that literature has stressed narrow fingers. These theoretical formulations incorporate a smooth cosine-dependent anisotropy term in the dynamical equation but tend to stress an expectation of narrow fingers, at least for some angles. None of these papers examine the stability of the narrow-finger solutions.

Ben Amar *et al.* [21] have recently published results from an experiment that may well be related to ours. They studied high-velocity fingering over a nylon mesh in a Hele-Shaw cell, and, after averaging over many flow realizations, constructed average-finger patterns with widths above the ST result. Since their individual flow patterns were very unstable and so far into the DLA-like regime, it is unclear how to compare their results with ours, which were obtained from stable and reproducible flows. Further caution in interpreting the similarities of the two experiments in producing fatter fingers is warranted because (1) for most of their data their capillary lengths are small compared to their lattice constants; (2) there may be differences due to the different wetting properties of nylon and glass, and (3) a stretched-nylon lattice may be less homogeneous and more deformable than the glass etched lattices specified in Table I.

In conjunction with their experiment, Ben Amar *et al.* performed a calculation, which indicates the existence of an "exceptional solution" when adverse anisotropy is added to the ST problem. They report that this exceptional solution is wider than the standard ST finger and becomes the selected solution above a threshold in $1/B$. More recently, Combescot [39] has extended the study of this exceptional solution at adverse anisotropy in the small surface tension (large $1/B$) limit, confirming the calculated results of Ben Amar *et al.* and arguing that the exceptional solution should become wider as $1/B$ is increased. Neither paper comments on the possibility of wider ST fingers at $\theta = 0°$. There is no obvious inconsistency between the present results and the work of Ben Amar *et al.* or Combescot, and further work may well show that their exceptional solution can be extended to explain our results.

Corvera, Guo, and Jasnow [40], using Hele-Shaw equations with an anisotropic surface tension and no kinetic term, have used both analytic and computational techniques to study finger width as a function of $1/B$ for two cases, one of which has surface tension, T, a local maximum at the ST fingertip and the other with T a local minimum at the finger tip. In the case where T is a local minimum at the finger tip, they find the selected solution to be indistinguishable from the normal ST finger. When T is a local maximum, the normal ST finger is also indistinguishable from their selected solution below a threshold in $1/B$. Above this threshold, they observe a selection of a finger wider than the ST finger.

In comparing our results with those predicted by Corvera *et al.*, we find consistency if we assume that T has a local maximum at the finger tip for flow at $\theta = 0°$. In that case, we contradict none of their results, since our square lattice has been measured at only 0° and 10°, and the T should only find its deepest minimum at 45°. Our rectangular lattice has been measured at 45°, but the twofold symmetry of the rectangular lattice might not be expected to cause T to reach the deepest local minimum until $\theta = 90°$. Thus our observation of the ST finger up to a threshold of about $1/B \approx 70$, followed by fatter fingers at larger values of $1/B$ bears a resemblance to the work of Corvera *et al.* Above some value of $1/B$, kinetic anisotropy should become important, and the results of Corvera *et al.* do not deal with this, so the eventual return of our data toward the ST value in no way contradicts their low $1/B$ results.

It should also be noted that the selection of finger widths dramatically different from the ST values does not set in abruptly at some very large value of the anisotropy. Rather, it appears smoothly as the anisotropy is increased, with small anisotropies ($a \leq 0.106$) yielding results indistinguishable from the ST values and larger values ($a \geq 0.18$) showing stronger effects as the anisotropy

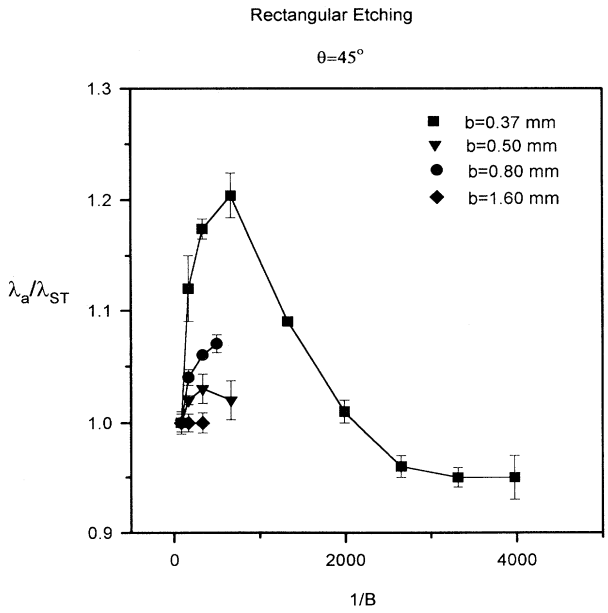

FIG. 5. Dimensionless ratio of perturbed-cell finger width to unperturbed-cell finger width vs $1/B$ for several values of cell gap, b, for the cell with the rectangular lattice. The lines shown are sketched to guide the eye.

increases. This is illustrated in Fig. 5, which shows the ratio of finger width to ST finger for several values of anisotropy for the rectangular lattice at $\theta = 45°$.

It is difficult to assess the relation between the present experiment and solidification. The present experiment achieves a ratio of capillary length to lattice-cell dimension of 25, whereas the analogous quantity in solidification is typically of order 1000. In addition, the boundary conditions are difficult to establish for the present case, the lack of difference between flow over the rectangular and the square lattices strongly suggests that the boundary conditions have a profound effect on the present case, and the available theoretical work with averaged anisotropy in the surface tension suggests narrowed fingers at some angles. However, this experiment involves the first test of the effect on the ST steady-state finger of a perturbation which is both local (which bubble and wire experiments are not) and "microscopic" in the sense of having $l_c/d > 1$. As a uniquely local and microscopic perturbation, its production of dramatically different selection than had been expected constitutes a challenge to our understanding of this fundamental growth problem. The smooth onset of the differences in the selection as anisotropy changes suggests a tractable problem even though its systematics had not been anticipated.

SUMMARY AND CONCLUSIONS

We have measured the selection of steady-state viscous fingers in Hele-Shaw cells, one of whose glass plates has been etched with a very regular lattice of squares or rectangles. The etched lattices perturb the Saffman-Taylor problem with an anisotropy whose strength can be varied by varying the cell gap. Over a wide range of observable finger-tip velocities, the capillary length of the flow, l_c, is much larger than the cell size of the lattice. In this condition, the perturbation can be said to be both local and microscopic, in principle, a very different condition from other perturbations whose channel-flow selection properties have been studied.

At each observed angle, θ (between the lattice orientation and the flow-channel orientation), and for both lattices, steady-state fingers are observed over a wide range of flow-rate control parameter, $1/B$. These fingers are always symmetric and centered in the flow channel, with tip curvatures which place them in the ST family. At the very lowest flow velocities, the fingers also have the width of normal ST fingers. Above a threshold, $1/B \approx 70$, the selected finger becomes wider than the ST solution selected in the unperturbed case and this wider-finger solution persists at all larger values of $1/B$ for which the capillary length is much larger than the unit cell size. The ratio of the wider finger to the unperturbed finger increases with the strength of the anisotropy (i.e., inversely with cell gap).

At much higher tip velocities where the lattice can no longer be considered microscopic, the finger widths return close to the unperturbed values, and both narrower and wider fingers are obtainable, depending on the angle θ. At these high velocities, flows over the square lattice become very unstable at large anisotropy while the rectangular lattice solutions are only very unstable at $\theta = 0°$.

ACKNOWLEDGMENTS

We appreciate helpful discussions with David Jasnow and Alain Karma. This work was supported by the DOE under Grant No. DE-FG02-84ER45131.

[1] R. Combescot, T. Dombre, V. Hakim, Y. Pomeau, and A. Pumir, Phys. Rev. Lett. **56**, 2036 (1986).
[2] D. C. Hong and J. Langer, Phys. Rev. Lett. **56**, 2032 (1986).
[3] B. I. Shraiman, Phys. Rev. Lett. **56**, 2028 (1986).
[4] J. M. Vanden-Broeck, Phys. Fluids **26**, 2033 (1983).
[5] D. A. Kessler and H. Levine, Phys. Rev. A **32**, 1930 (1986).
[6] S. Tanveer, Phys. Fluids **30**, 1589 (1987).
[7] D. A. Kessler and H. Levine, Phys. Fluids **30**, 1246 (1987).
[8] Y. Couder, O. Cardoso, D. Dupuy, P. Tavernier, and W. Thom, Europhys. Lett. **2**, 437 (1986).
[9] Y. Couder, N. Gerard, and M. Rabaud, Phys. Rev. A **34**, 5175 (1986).
[10] V. Horvath, T. Vicsek, and J. Kertesz, Phys. Rev. A **35**, 2353 (1987).
[11] G. Zocchi, B. Shaw, A. Libchaber, and L. Kadanoff, Phys. Rev. A **36**, 1894 (1987).
[12] M. Rabaud, Y. Couder, and N. Gerard, Phys. Rev. A **37**, 935 (1988).
[13] M. Matsushita and H. Yamada, J. Cryst. Growth **99**, 161 (1990).
[14] H. Thome, R. Combescot, and Y. Couder, Phys. Rev. A **41**, 5739 (1990).
[15] J. Yokoyama, Y. Kitagawa, H. Yamada, and M. Matsushita, Physica A **204**, 789 (1993).
[16] E. Ben-Jacob, R. Godbey, N. Goldenfeld, J. Koplik, H. Levine, T. Mueller, and L. M. Sander, Phys. Rev. Lett. **55**, 1315 (1985).
[17] J. D. Chen, Exp. Fluids **5**, 363 (1987).
[18] E. Ben-Jacob, P. Garik, T. Mueller, and D. Grier, Phys. Rev. A **38**, 1370 (1988).
[19] Y. Couder, F. Argoul, A. Arneodo, J. Maurer, and M. Rabaud, Phys. Rev. A **42**, 3499 (1990).
[20] Y. Couder, S. Michalland, M. Rabuad, and H. Thome, in *Nonlinear Evolution of Spacio-temporal Structures in Dissipative Continuous Systems*, edited by F.H. Busse and L. Kramer (Plenum Press, New York, 1990).
[21] M. Ben Amar, R. Combescot, and Y. Couder, Phys. Rev. Lett. **70**, 3047 (1993).
[22] D. A. Kessler, J. Koplik, and H. Levine, Phys. Rev. A **34**, 4980 (1986).
[23] A. T. Dorsey and O. Martin, Phys. Rev. A **35**, 3989 (1987).
[24] D. C. Hong and J. S. Langer, Phys. Rev. A **36**, 2325

(1987).
[25] G. Li, D. Kessler, and L. Sander, Phys. Rev. A **34**, 4551 (1986).
[26] D. C. Hong, Phys. Rev. A **37**, 2724 (1988).
[27] R. Combescot and T. Dombre, Phys. Rev. A **39**, 3525 (1989).
[28] D. C. Hong, Phys. Rev. A **39**, 2042 (1989).
[29] B. E. Shaw, Phys. Rev. A **40**, 5875 (1989).
[30] H. Guo and D. Hong, Phys. Rev. A **41**, 2995 (1990).
[31] D. C. Hong, Phys. Rev. A **43**, 5199 (1991).
[32] R. Almgren (private communication).
[33] J. Pitts, J. Fluid Mech. **97**, 53 (1980).
[34] P. Tabeling, G. Zocchi, and A. Libchaber, J. Fluid Mech. **177**, 67 (1987).
[35] C. Park and G. M. Homsy, J. Fluid Mech. **139**, 291 (1984).
[36] P. Tabeling and A. Libchaber, Phys. Rev. A **33**, 794 (1986).
[37] D. Bensimon, Phys. Rev. A **33**, 1302 (1986).
[38] S. Sarkar and D. Jasnow, Phys. Rev. A **39**, 5299 (1989).
[39] R. Combescot, Phys. Rev. E **49**, 4172 (1994).
[40] E. Corvera, H. Guo, and D. Jasnow (private communication).